nanoenergy advances

MDPI

Review

Recent Advances in Lubricant-Based Triboelectric Nanogenerators for Enhancing Mechanical Lifespan and Electrical Output

Seh-Hoon Chung [1], Jihoon Chung [2,*] and Sangmin Lee [1,*]

[1] School of Mechanical Engineering, Chung-Ang University, 84 Heukseok-ro, Dongjak-gu, Seoul 06974, Korea; sehhoon1010@cau.ac.kr
[2] Department of Chemical & Biomolecular Engineering, University of California, Berkeley, CA 94720, USA
* Correspondence: jihoon05@berkeley.edu (J.C.); slee98@cau.ac.kr (S.L.)

Abstract: A triboelectric nanogenerator (TENG) is a noteworthy mechanical energy harvester that can convert mechanical energy into electricity by combining triboelectrification and electrostatic induction. However, owing to the nature of its working mechanism, TENGs have critical limitations in mechanical and electrical aspects, which prevent them from being utilized as primary power sources. To overcome these limitations, several studies are turning their attention to utilizing lubricants, which is a traditional method recently applied to TENGs. In this review, we introduce recent advances in lubricant-based TENGs that can effectively enhance their electrical output and mechanical lifespan. In addition, this review provides an overview of lubricant-based TENGs. We hope that, through this review, researchers who are trying to overcome mechanical and electrical limitations to expand the applications of TENGs in industries will be introduced to the use of lubricant materials.

Keywords: triboelectric nanogenerator; energy harvesting; lubricant liquid; output enhancement; mechanical lifespan

Citation: Chung, S.-H.; Chung, J.; Lee, S. Recent Advances in Lubricant-Based Triboelectric Nanogenerators for Enhancing Mechanical Lifespan and Electrical Output. *Nanoenergy Adv.* **2022**, *2*, 210–221. https://doi.org/10.3390/nanoenergyadv2020009

Academic Editors: Ya Yang and Zhong Lin Wang

Received: 18 April 2022
Accepted: 13 May 2022
Published: 19 May 2022

1. Introduction

As the number of portable electronics and Internet of Things (IoT) devices has increased drastically, the need for on-site energy generation has been in the spotlight to power these devices individually and extend their battery life. Energy-harvesting technologies can convert ambient energy, such as solar [1–3], wind [4–8], wave [9–12], and radio frequency [13–15], into electricity that can provide sufficient energy for small electronic devices. Among these energy-harvesting technologies, harvesting mechanical energy has great potential to effectively power portable and small electronics because it is not affected by external environment such as weather conditions. In order to harvest mechanical motion, energy harvesters that utilizes electromagnetic, piezoelectric effect has been utilized [16,17]. Triboelectric nanogenerators (TENGs) are one of mechanical energy harvesters that can generate electricity by combining triboelectrification and electrostatic induction [18–23]. Owing to their light weight [24], high electrical output [25,26], and availability of raw materials, recent research has focused on developing various TENG designs and structures to effectively collect energy from multiple mechanical sources, such as vibration energy [27–30] and rotation energy [31–34]. Currently, TENGs charge commercial electrical devices and lithium-ion batteries used in building self-powered systems [35–38] and are enhanced for utilization in industrial applications [39].

However, the working mechanisms of TENGs are critically limited in their mechanical and electrical aspects, restricting the use of TENGs as primary power sources. From a mechanical perspective, TENGs have two materials placed in contact to cause triboelectricity, leading to frictional wear. Frictional wear is one of the constant limitations of TENGs because they generate electrical output through mechanical input [40]. Due to the nature of triboelectricity, surface friction from two or more material is necessary to generate surface

charge and requires consistent or periodical contact due to degradation of surface charge over time. Particularly, various TENGs utilizing micro-/nano-structures and polymer dielectric materials for surface charge enhancements are more vulnerable to frictional wear owing to their poor mechanical properties [41,42]. Frictional damage on a TENG surface leads to a decrease in electrical output due to surface structure failure as well as device failure when mechanical damage is accumulated.

An electrical limitation is imposed when the surface charge potential of the material is higher than the breakdown potential of air, as the surface charge is lost through field emission and ionization of air [43–45]. Since more and more studies report higher surface charge materials with surface micro and nanostructures, this electrical limitation is becoming restriction factor for developing high power TENG [46,47]. With the introduction of the upper limitation of surface charge due to air breakdown, there have been studies in favor and opposing the use of this phenomenon to enhance the electrical output of TENGs [48–50]. However, the cause of this limitation remains unresolved, as the primary potential difference of TENGs is governed by the surface charge, which is still limited by air breakdown. Therefore, to overcome these limitations, several studies are turning their attention to utilizing lubricants, a traditional method recently applied to TENGs, to overcome both limitations.

In this review, we highlight recent advances in lubricant-based TENGs that can effectively enhance both the electrical output and mechanical lifespan of TENGs. The review will focus on overviewing lubricant-based TENGs, their working mechanisms, their various designs, and an output comparison with conventional TENGs. Especially, the reason for lubricant based TENGs can overcome mechanical and electrical limitation of TENG, and experimental data from various studies will be discussed. Finally, the different perspectives regarding lubricant-based TENGs, and challenges associated with their use are discussed.

2. Lubricant-Based TENGs

When mechanical input is applied to a conventional TENG, two dielectric materials come into contact and cause triboelectrification [51–57]. The surface charge generated by the friction between the two dielectric materials is then transferred to the electrodes through electrostatic induction [58–63]. Contact between the dielectric materials is inevitable during this process, leading to frictional wear. The frictional wear gradually decreases the output of TENG by damaging the surface structure fabricated on the surface and eventually fails after the mechanical damage is accumulated. Therefore, utilizing lubricants between the frictional surfaces is an effective approach to reducing the frictional force. Moreover, lubricating oils such as transformer oil and vegetable oil are also called as dielectric liquid which can be used as insulating material by its high breakdown voltage [64]. As the surface charge of dielectric materials in TENGs can be released to the atmosphere, utilizing the lubricant at TENGs can increase the electrical output. By these effects, recently, various lubricant materials combined with mechanical designs have been introduced to overcome the mechanical limitations of TENGs (Figure 1). As sliding motion-based TENGs are more vulnerable to friction failure, lubricant materials were more actively utilized in these than in other TENGs, such as horizontal contact-separation modes.

As shown in Figure 1a, a lubricating liquid can be applied to a sliding motion-based TENG system [65]. The lubricant liquid on the TENG surface forms a thin layer that can effectively decrease the frictional force between the electrode and polytetrafluoroethylene (PTFE) surface. The main electrical potential difference is generated by friction between the PTFE and polystyrene (PS) surfaces, and the TENG generates an amplified current of over 1 mA because the dielectric liquid acts as a switch during operation. Furthermore, field emission occurs when the PTFE contacts the electrode surface, and electrons can flow directly from the PTFE surface to the electrode. Hence, the lubricant liquid enhanced the electrical output of the TENG by suppressing air breakdown. Various TENGs utilizing other lubricant liquids, such as oleic acid, have been introduced (Figure 1b). In a previous study, oleic acid and PS were dissolved in N,N-dimethylformamide, and then spin-coated

on the conductive polyimide (PI) surface to be paired with nylon-11 surface [66]. In this work, the negative surface charge is generated on oleic acid and PS solution and positive surface charge is generated on nylon surface. The surface charge of PS and nylon is induced to the copper electrode which is underlying each material. The vertical movement between these materials generate electric potential difference which leads to generating electrical output. A similar structure is shown in Figure 1c, where squalene liquid was applied to the TENG surface [67]. The squalene liquid, which was chosen to be most effective through experiment with various liquids, provides a thin layer that can effectively lower friction and increase the surface charge, enhancing electrical output. The main surface charge is generated on the PI surface of the TENG and generates electrical output through horizontal movement. It is also possible to utilize liquids such as hexadecane, as shown in Figure 1d, where the nylon surface was coated with hexadecane to form a hexadecane-containing sandwich structure [68]. In this work, traditional triboelectric material consisting of PTFE and nylon was chosen to generate negative and positive surface charge, respectively. A total of 5 mL of hexadecane was brushed to the surface to form a hexadecane-containing sandwich structure.

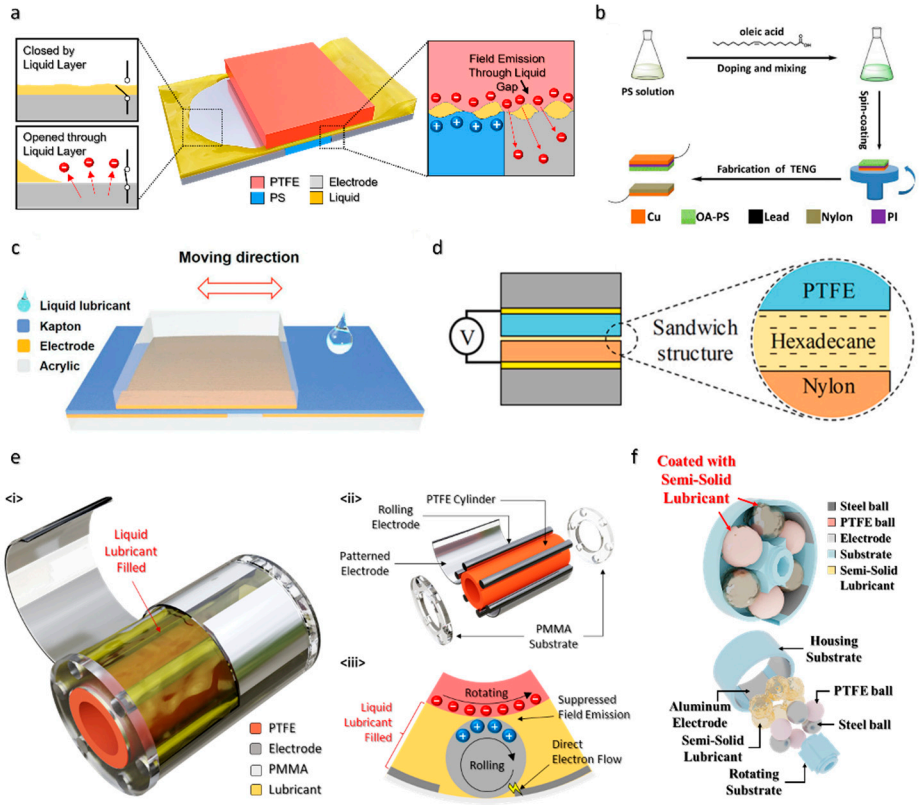

Figure 1. Various designs for lubricant-based TENGs. Schematic of lubricant-based TENG using: (**a**) dielectric lubricant (Reprinted with permission from ref. [65]. 2021, Elsevier); (**b**) oleic acid (Reprinted with permission from ref. [66]. 2020, Elsevier); (**c**) liquid lubricant (Reprinted with permission from ref. [67]. 2020, Wiley); (**d**) hexadecane sandwich structure (Reprinted with permission from ref. [68]. 2021, Elsevier); (**e**) rolling cylinder structure (Reprinted with permission from ref. [69]. 2021, Wiley); (**f**) ball-bearing structure (Reprinted with permission from ref. [70]. 2022, Elsevier).

Recent research has focused on combining mechanical design with lubrication to enhance the mechanical lifespan of TENGs. As shown in Figure 1e, a TENG coated with a non-polar liquid lubricant consists of an outer cylinder substrate, multiple rolling electrodes, a PTFE cylinder, and aluminum plate electrodes placed on the inner surface of the cylinder substrate [69]. The rolling electrodes rotating inside the cylinder substrate have rolling friction, which is considerably lower than sliding friction. The main electrical potential

difference is generated through PTFE and rolling aluminum electrode in this study. The electrical potential accumulated in the rolling aluminum electrode is then transferred to the plate electrode as the rolling electrode rotates due to external mechanical input. In addition, the entire TENG system was submerged in a liquid lubricant, which enhanced the mechanical lifespan. With the lubricant-applied design, the aluminum surface of this TENG had no frictional damage even after 72 h of continuous operation. In addition, as shown in Figure 1f, a ball-bearing TENG with a semi-solid lubricant such as grease was introduced. A commercial semi-solid lubricant (multipurpose lubricant, Super Lube®), which can be used under a wide range of environmental conditions, was applied to the TENG surface [70]. The main electrical potential difference is generated through PTFE and steel ball located inside the substrate casing, and through commercial semisolid lubricant, it can effectively lower friction between each surface; additionally, rolling friction significantly lowered the friction force compared with sliding friction.

3. Working Mechanism of Lubricant-Based TENGs

The lubricant liquid on the TENG surface can enhance the mechanical and electrical performance. From a mechanical perspective, lubricant liquid can effectively decrease the frictional wear of TENGs in various condition. There are four different lubrication regimes which are called as boundary lubrication, mixed lubrication, full film lubrication and elastohydrodynamic lubrication. Each regimes show different result of frictional damage and it is decided by several factors such as dynamic viscosity of the lubricant liquid, entrainment speed, normal load per the length of contact, and the contact condition [71]. Normally the contact surfaces are less damaged by the full film lubrication which is also called as hydrodynamic lubrication. By full film lubrication, a sufficient amount of lubricant liquid between two surfaces can form a fluid film that can minimize the frictional wear between them [72]. Due to the fluid film, the two contact surfaces can be separated, thus the frictional wear effectively decreases. Furthermore, through elastohydrodynamic lubrication, the frictional wear from rolling friction can be decreased [73]. Even though rolling friction cause less wear than sliding friction, it can also be improved by using lubricant liquid. As both the coefficient of rolling friction by the roughness of the rolling surface and the contact surface, and normal force, cause friction force, the wear of the rolling surface and contact surface also occurs. Moreover, in real life, the slip between the rolling surface and contact surface can be also occurred. If the accurate lubricant liquid is used, due to the elastohydrodynamic lubrication, lubrication liquid can reduce the frictional damage of various devices such as bearing or gear. Additionally, lubricant liquid can also reduce heat from the friction and prevent the damage from the wear particles [74]. Hence, lubricant liquid has numerous advantages to be utilized for the TENGs. Considering that TENGs, especially those that harvest sliding motion, are constantly exposed to frictional contact, combining a lubricated surface and low-friction mechanical design is essential for a longer lifespan and expanding the application of TENGs to primary power sources.

Along with the mechanical advantages of applying a lubricant to TENGs, the electrical output can be enhanced by lubricating the TENG surface. As the electrical output of TENGs is governed by the amount of surface charge on the dielectric material, enhancing the surface charge is an important factor in increasing the total electrical output. However, as the air breakdown voltage is commonly known to be 3×10^6 V/m [75], dielectric surfaces with electrical potentials higher than this value can cause field emission and air breakdown, where electrons on the dielectric surface can escape to the air. Due to the electrons escaping from the material surface, the surface charge of the material surface is restricted as well. This leads to an upper limitation of the surface charge when the TENG operates in an atmospheric environment, resulting in reduced electrical output [43]. As more and more studies are reporting high surface charge materials and device structures to be utilized in TENG, overcoming this restriction is becoming important [76–78]. Surfaces under a lubricant liquid can avoid field emission and air breakdown because the lubricant liquid tends to have a higher breakdown voltage than air [79]. As shown in Figure 2a,

under atmospheric conditions, electrons can escape to air owing to field emission and air breakdown, which would limit the maximum surface charge. This indicates that by utilizing lubricant, dielectric surface can withhold more surface charge compared to when it is exposed to air. Moreover, the liquid lubricant can be polarized due to the surface charge, resulting in transferring the charge to the electrode by electrostatic induction. As shown in Figure 2b, the voltage and current measured increased when the steel sphere was sliding over a polyvinylidene fluoride (PVDF) surface and polyalphaolefin (PAO) 4 was applied between them [80]. PAO 4 fills the microscale gap between the PVDF and steel sphere surfaces. Hence, the air breakdown at the contact interface was inhibited, and the triboelectric charge of PVDF was preserved because of the low polarity and high dielectric constant of PAO 4.

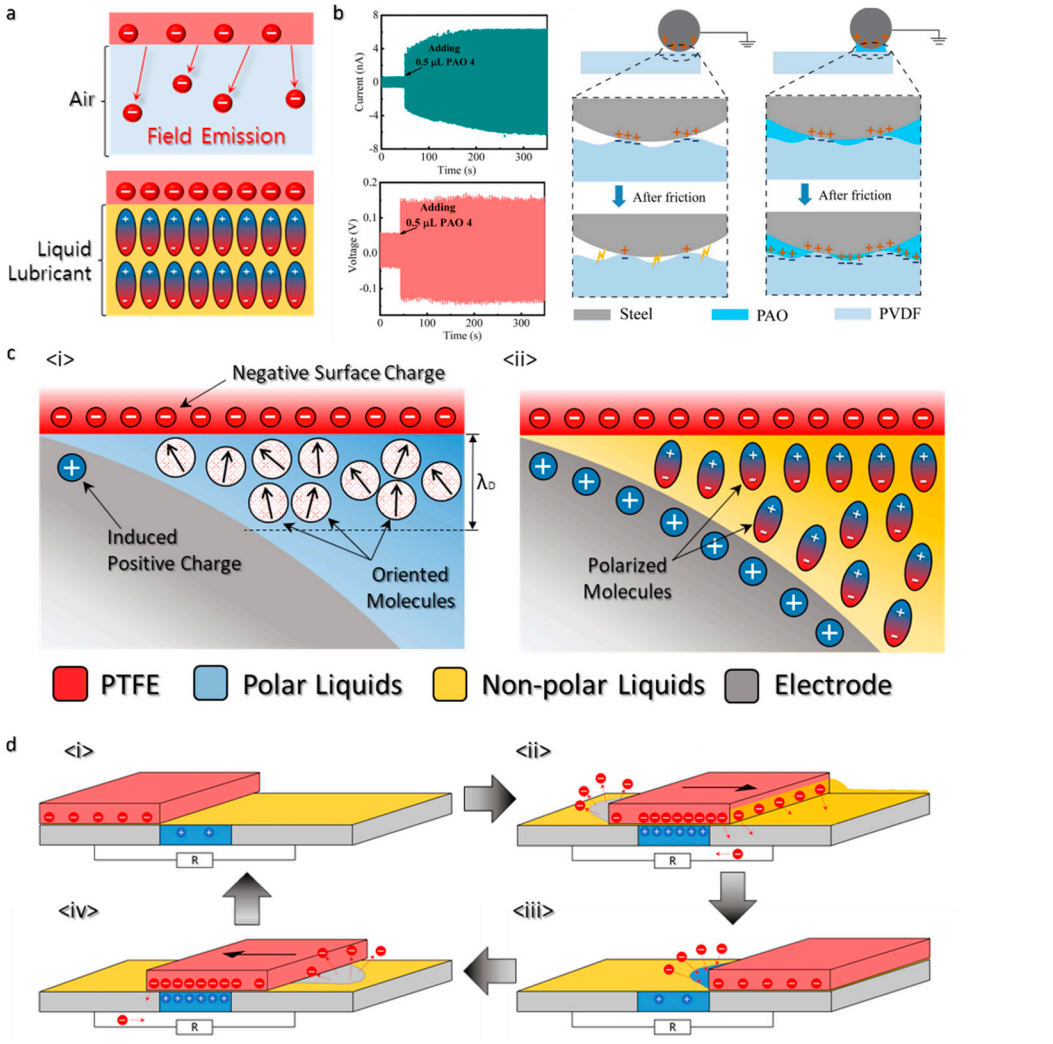

Figure 2. Working mechanism of lubricant-based TENGs: (**a**) schematic of a liquid lubricant suppressing air breakdown (Reprinted with permission from ref. [65]. 2021, Elsevier); (**b**) effect of adding lubricant on dielectric surface and schematic of liquid lubricant suppressing air breakdown in a microscale gap (Reprinted with permission from ref. [80]. 2022, Elsevier); (**c**) comparison of polar and non-polar liquid transferring surface charge to the electrode (Reprinted with permission from ref. [69]. 2021, Wiley); (**d**) accumulated charge on the dielectric material transfers to the electrode, producing amplified output (Reprinted with permission from ref. [65]. 2021, Elsevier).

Electrostatic induction plays an important role in the working mechanism of the TENGs for transferring the surface charge to the electrode. However, when the liquid is in contact with the surface of the dielectric material, it forms an electrical double layer

(EDL), which screens the surface charge of the solid material. This means that the surface charge is reduced by EDL and surface charge cannot be transferred to the electrode by electrostatic induction. Hence, the electrical output is suppressed as the electrical potential difference between the electrode and dielectric material with the surface charge is reduced. As shown in Figure 2c, when polar liquids, such as water and ethanol, come into contact with the solid surface with the surface charge, the charge is screened by oriented liquid molecules [81]. The characteristic distance where the charge is screened by contacting liquid is called the Debye length (λ_D). When a strong polar liquid such as water comes into contact with the dielectric surface, λ_D can be <20 nm [82]. Even ethanol, which has a lower polarity compared with water, has λ_D around 38 nm. This indicates that a liquid with a lower λ_D will screen the surface charge even with nano- to micro-scale gaps, resulting in a substantial decrease in the electrical output by reducing the charge induced to the TENG electrodes. This would result in a decrease in electrical output. In contrast, non-polar liquids have a higher λ_D over 1 μm, which is significantly higher than that of polar liquids; therefore, a higher surface charge can be induced on the electrode through the polarization of the non-polar liquid molecules without electrical screening.

By lubricant liquid effectively suppressing air breakdown and inducing more charge, it can also open a new working mechanism for TENG by introducing a combination of lubricant suppressing air breakdown and non-lubricated surfaces inducing air breakdown. Figure 2d shows the extended working mechanism of the lubricant-based TENG, which utilizes the accumulated charge due to the non-polar lubricant liquid. When the PTFE plate slides across the PS surface, negative and positive charges are generated on the PTFE and PS surfaces, respectively, because of the triboelectric effect between the two surfaces. As the PTFE plate comes in contact with the electrode, electrons on the PTFE surface are emitted to the plate electrode and electrons from the counter electrode are emitted into the air, owing to the field emission. As field emission occurs on both electrodes, it can produce a high electrical output. In this working mechanism, the TENG is able to produce high electrical output through a combination of lubricant suppressing air breakdown on the solid surface, and the air-exposed surface inducing air breakdown to allow more electrons to flow between the two plate electrodes. As the PS surface reverses its sliding motion, a contrasting electrical output is produced, owing to the reverse field emission. As shown in this figure, lubricant materials are being actively studied in the TENG field, and new working mechanisms to enhance the electrical output of TENG have yet to be discovered.

4. Performance of Lubricant-Based TENGs and Relevant Parameters

Figure 3a,b show the mechanical advantages of utilizing lubricants in TENGs. As shown in Figure 3a, the microscopic photograph suggests that the TENG electrode surface remained undamaged in a lubricated environment even after continuous operation for 72 h [69]. This study also reports that the surface under non-lubricated environment have shown surface damages with noticeable scratches under microscope. In addition to reducing the frictional force and wear, the TENG surface may be subjected to less thermal damage during operation. Figure 3b shows the photograph of the TENG surface, and the thermal image during operation which shows the thermal condition and surface damage of the ball-bearing TENG [70]. When a semi-solid lubricant was applied to the surface, the TENG showed only a 1.7 °C increase in temperature after 55 h of continuous operation, and there was no noticeable electrode damage except for the dent marks from the rotating ball-bearing spheres. In contrast, when no lubricant was applied to the surface, the operating temperature rises to a maximum of 69.2 °C after 1 h of operation. In addition, it showed noticeable damage to the electrode with metal powder wear from the electrode surface compared with a ball-bearing TENG with a semi-solid lubricant. The lower operation temperature shows that the friction force is much less in lubricated condition compared to non-lubricated condition. Through a lower operation temperature, the materials can have less damage from mechanical motion as well. In terms of electrical output, Figure 3c,d show the transferred charge and current output, respectively, depending on the presence of a

lubricant liquid on the surface. The transferred charge and current of the lubricated TENG were more than twice compared with those of the TENG operated in air. As mentioned in the previous paragraphs, this is result from combination of suppressing air breakdown and increasing the Debye length through using non-polar liquid lubricant.

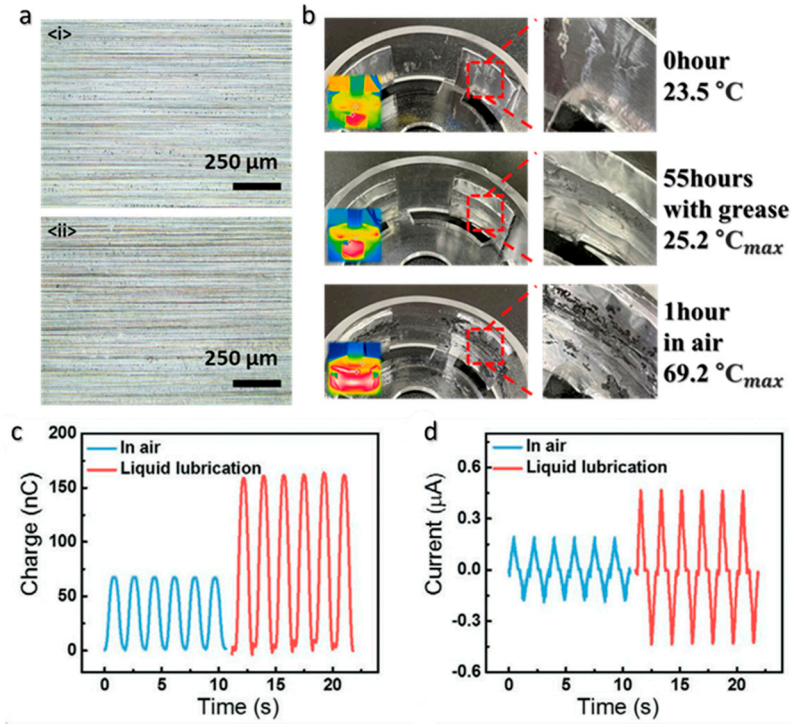

Figure 3. Mechanical and electrical performance of lubricant-based TENGs: (**a**) microscopic photograph of electrode surface <**i**> before and <**ii**> after 72 h of continuous operation of the TENG (Reprinted with permission from ref. [69], 2021, Wiley); (**b**) photograph of the electrode surface and the thermal image of TENG during operation (Reprinted with permission from ref. [70]. 2022, Elsevier); (**c**) transferred charge; (**d**) current output of TENG with and without liquid lubrication (Reprinted with permission from ref. [67]. 2020, Wiley).

To further enhance the mechanical lifespan and electrical output, future studies are required to optimize the lubricants specialized for TENG applications. One of the important steps for optimizing lubricant materials is a quantitative study of various liquid lubricants. Many studies are continuing this effort to provide guideline for selecting appropriate lubricant materials to be utilized in various applications. As shown in Figure 4a,b, a recent study showed that liquid lubricants such as squalene, paraffin oil, and PAO 10 have higher electrical outputs than TENG operated under dry conditions [83]. In this work, TENG operating with liquids such as olive oil, rapeseed oil, plurial A 500 PE, PEG 200, water have shown considerably lower electrical output. This study also reported that the relative permittivity and viscosity of lubricant is the key factor to increase output of TENG according to the experimental result. In addition, in other studies, lubricant liquids such as mineral oil and silicone oil show high electrical output, whereas castor oil, water, and ethanol show relatively low output (Figure 4c,d). Overall, various studies have shown that synthetic non-polar liquids such as squalene, mineral oil, silicone oil, and hexadecane have a higher electrical output, whereas polar liquids such as ethylene glycol, water, and ethanol tend to show low electrical output. As shown in Figure 2, the polar liquids screen the surface charge and lead to a decrease in the output. In addition, considering that organic oils such as rapeseed, olive, and castor oils are mixtures of various compounds, they contain polar molecules such as glycerol that would lower the electrical output of TENGs. As shown in Figure 4e–h, a study on the electrical output and friction coefficient depending on PAO 4, perfluoropolyether (PFPE), glycerol, and ethanol, respectively. As shown in the plots, the

electrical output increases and friction coefficient decreases when using a non-polar liquid such as PAO 4 and PFPE, whereas the electrical output decreases and friction coefficient increases when using polar liquid such as glycerol and ethanol. Considering that there are vast number of synthetic and natural oils are used for lubrication, there must be further studies on these materials as well as effect of these lubrication materials when lubrication materials are used for a longer extension of time.

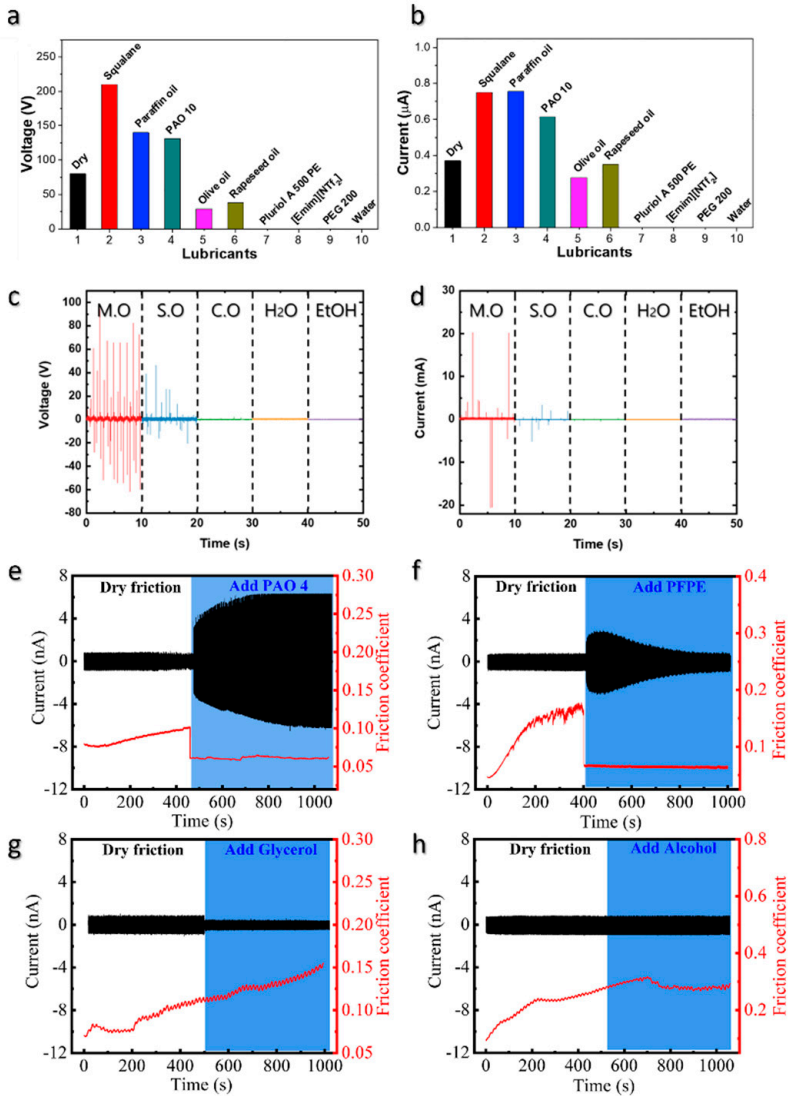

Figure 4. Electrical output depending on various liquids applied on the surface of TENGs: (**a**,**c**) Voltage and (**b**,**d**) current output of TENGs depending on various liquids (Reprinted with permission from ref. [69]. 2021, Wiley. And reprinted with permission from ref. [83]. 2021, Elsevier). Measured current and friction coefficient when (**e**) PAO 4, (**f**) PFPE, (**g**) glycerol, and (**h**) alcohol was applied on the surface of TENGSs.

5. Summary and Perspectives

This review introduces the current strategies and an overview of lubrication-based TENGs. As the air breakdown effect limits the electrical performance and induces frictional wear affecting the mechanical lifespan of TENGs, the use of lubricants has been actively studied to overcome these limitations. These studies have shown that a lubricant liquid applied to the TENG surface can effectively increase the mechanical lifespan and electrical output by lowering the friction coefficient and suppressing air breakdown. Previous studies have shown working mechanism of lubricant-based TENGs can generate high electrical

output through suppressing air breakdown and non-polar liquid with high Debye length, which would effectively transfer the surface charge through electrostatic induction. Various mechanical designs and working mechanisms have been developed to further decrease the friction force and enhance the electrical output. For further enhancement of lubricant-based TENGs, optimization of lubricant liquids and mechanical components should be considered at the design level, and additional quantitative studies are required as follows:

(1) Optimization of lubricant-based TENG design to withhold more lubricant on the surface during operation and advanced surface design considering lubrication at the design level;
(2) Further quantitative analysis of the relationship between TENGs and lubricant liquids, especially on the EDL formation of lubricant liquids under high surface charge conditions;
(3) Quantitative analysis of various lubricant liquids affecting mechanical lifespan and electrical output of TENG, including commercial synthetic and organic oil;
(4) Long-term influence of lubricant liquids on TENG surfaces and the effect of long-term operation on polymer surfaces.

We hope that, through this review, researchers who are trying to overcome mechanical and electrical limitations for expanding the applications of TENGs in industries will be introduced to the use of lubricant materials. We believe that constant research efforts and innovations in lubricant-based TENG have great potential for utilizing TENGs as a primary energy source for existing electronics.

Author Contributions: Conceptualization, S.-H.C., J.C. and S.L.; writing—original draft preparation, S.-H.C.; writing—review and editing, J.C. and S.L.; supervision, J.C. and S.L.; project administration, S.L.; funding acquisition, J.C. All authors have read and agreed to the published version of the manuscript.

Funding: This research was supported by Basic Science Research Program through the National Research Foundation of Korea(NRF) funded by the Ministry of Education(2021R1A6A3A03040052) and the National Research Foundation of Korea(NRF) grant funded by the Korea government(MSIT)(No. 2021R1A4A3030268).

Conflicts of Interest: The authors declare no conflict of interest.

References

1. Chalasani, S.; Conrad, J.M. A survey of energy harvesting sources for embedded systems. In Proceedings of the 2008 IEEE Southeastcon, Huntsville, AL, USA, 3–6 April 2008; pp. 442–447. [CrossRef]
2. Raghunathan, V.; Kansal, A.; Hsu, J.; Friedman, J.; Srivastava, M. Design considerations for solar energy harvesting wireless embedded systems. In Proceedings of the IPSN 2005, Fourth International Symposium on Information Processing in Sensor Networks, Boise, ID, USA, 15 April 2005; pp. 457–462.
3. Abdin, Z.; Alim, M.; Saidur, R.; Islam, M.; Rashmi, W.; Mekhilef, S.; Wadi, A. Solar energy harvesting with the application of nanotechnology. *Renew. Sustain. Energy Rev.* **2013**, *26*, 837–852. [CrossRef]
4. Li, S.; Yuan, A.J.; Lipson, H. Ambient wind energy harvesting using cross-flow fluttering. *J. Appl. Phys.* **2011**, *109*, 026104. [CrossRef]
5. Tan, Y.K.; Panda, S.K. Optimized wind energy harvesting system using resistance emulator and active rectifier for wireless sensor nodes. *IEEE Trans. Power Electron.* **2010**, *26*, 38–50.
6. Tan, Y.K.; Panda, S.K. Measurement. Self-autonomous wireless sensor nodes with wind energy harvesting for remote sensing of wind-driven wildfire spread. *IEEE Trans. Instrum. Meas.* **2011**, *60*, 1367–1377. [CrossRef]
7. Lee, J.-S.; Yong, H.; Choi, Y.I.; Ryu, J.; Lee, S. Stackable Disk-Shaped Triboelectric Nanogenerator to Generate Energy from Omnidirectional Wind. *Int. J. Precis. Eng. Manuf. Technol.* **2021**, *9*, 557–565. [CrossRef]
8. Yong, H.; Chung, J.; Choi, D.; Jung, D.; Cho, M.; Lee, S. Highly reliable wind-rolling triboelectric nanogenerator operating in a wide wind speed range. *Sci. Rep.* **2016**, *6*, 33977. [CrossRef]
9. Carrara, M.; Cacan, M.R.; Toussaint, J.; Leamy, M.J.; Ruzzene, M.; Erturk, A. Metamaterial-inspired structures and concepts for elastoacoustic wave energy harvesting. *Smart Mater. Struct.* **2013**, *22*, 065004. [CrossRef]
10. Khan, T.A.; Alkhateeb, A.; Heath, R.W. Millimeter Wave Energy Harvesting. *IEEE Trans. Wirel. Commun.* **2016**, *15*, 6048–6062. [CrossRef]

11. Younesian, D.; Alam, M.-R. Multi-stable mechanisms for high-efficiency and broadband ocean wave energy harvesting. *Appl. Energy* **2017**, *197*, 292–302. [CrossRef]
12. Chung, J.; Heo, D.; Shin, G.; Chung, S.-H.; Hong, J.; Lee, S. Water behavior based electric generation via charge separation. *Nano Energy* **2020**, *82*, 105687. [CrossRef]
13. Le, T.; Mayaram, K.; Fiez, T. Efficient Far-Field Radio Frequency Energy Harvesting for Passively Powered Sensor Networks. *IEEE J. Solid-State Circuits* **2008**, *43*, 1287–1302. [CrossRef]
14. Masotti, D.; Costanzo, A.; Del Prete, M.; Rizzoli, V. Genetic-based design of a tetra-band high-efficiency radio-frequency energy harvesting system. *IET Microw. Antennas Propag.* **2013**, *7*, 1254–1263. [CrossRef]
15. Zungeru, A.M.; Ang, L.-M.; Prabaharan, S.; Seng, K.P. Radio Frequency Energy Harvesting and Management for Wireless Sensor Networks. In *Green Mobile Devices and Networks: Energy Optimization and Scavenging Techniques*; CRC Press: Boca Raton, FL, USA, 2012; pp. 341–368.
16. Beeby, S.P.; Torah, R.N.; Tudor, M.J.; Glynne-Jones, P.; O'Donnell, T.; Saha, C.R.; Roy, S. A micro electromagnetic generator for vibration energy harvesting. *J. Micromech. Microeng.* **2019**, *17*, 1257–1265. [CrossRef]
17. Lefeuvre, E.; Badel, A.; Richard, C.; Petit, L.; Guyomar, D. A comparison between several vibration-powered piezoelectric generators for standalone systems. *Sens. Actuators A Phys.* **2006**, *126*, 405–416. [CrossRef]
18. Zhu, G.; Pan, C.; Guo, W.; Chen, C.-Y.; Zhou, Y.; Yu, R.; Wang, Z.L. Triboelectric-Generator-Driven Pulse Electrodeposition for Micropatterning. *Nano Lett.* **2012**, *12*, 4960–4965. [CrossRef] [PubMed]
19. Wang, S.; Lin, L.; Wang, Z.L. Nanoscale Triboelectric-Effect-Enabled Energy Conversion for Sustainably Powering Portable Electronics. *Nano Lett.* **2012**, *12*, 6339–6346. [CrossRef]
20. Jang, S.; Joung, Y.; Kim, H.; Cho, S.; Ra, Y.; Kim, M.; Ahn, D.; Lin, Z.-H.; Choi, D. Charge transfer accelerating strategy for improving sensitivity of droplet based triboelectric sensors via heterogeneous wettability. *Nano Energy* **2022**, *97*, 107213. [CrossRef]
21. Kim, M.; Ra, Y.; Cho, S.; Jang, S.; Kam, D.; Yun, Y.; Kim, H.; Choi, D. Geometric gradient assisted control of the triboelectric effect in a smart brake system for self-powered mechanical abrasion monitoring. *Nano Energy* **2021**, *89*, 106448. [CrossRef]
22. Chung, J.; Cho, H.; Yong, H.; Heo, D.; Rim, Y.S.; Lee, S. Versatile surface for solid–solid/liquid–solid triboelectric nanogenerator based on fluorocarbon liquid infused surfaces. *Sci. Technol. Adv. Mater.* **2020**, *21*, 139–146. [CrossRef]
23. Wu, C.; Wang, A.; Ding, W.; Guo, H.; Wang, Z.L. Triboelectric Nanogenerator: A Foundation of the Energy for the New Era. *Adv. Energy Mater.* **2018**, *9*, 1802906. [CrossRef]
24. Ra, Y.; Oh, S.; Lee, J.; Yun, Y.; Cho, S.; Choi, J.H.; Jang, S.; Hwang, H.J.; Choi, D.; Kim, J.-G.; et al. Triboelectric signal generation and its versatile utilization during gear-based ordinary power transmission. *Nano Energy* **2020**, *73*, 104745. [CrossRef]
25. Liu, Y.; Liu, W.; Wang, Z.; He, W.; Tang, Q.; Xi, Y.; Wang, X.; Guo, H.; Hu, C. Quantifying contact status and the air-breakdown model of charge-excitation triboelectric nanogenerators to maximize charge density. *Nat. Commun.* **2020**, *11*, 1599. [CrossRef] [PubMed]
26. Chung, J.; Heo, D.; Shin, G.; Choi, D.; Choi, K.; Kim, D.; Lee, S. Ion-Enhanced Field Emission Triboelectric Nanogenerator. *Adv. Energy Mater.* **2019**, *9*, 1901731. [CrossRef]
27. Kim, D.; Chung, J.; Heo, D.; Chung, S.; Lee, G.; Hwang, P.T.J.; Kim, M.; Jung, H.; Jin, Y.; Hong, J.; et al. AC/DC Convertible Pillar-Type Triboelectric Nanogenerator with Output Current Amplified by the Design of the Moving Electrode. *Adv. Energy Mater.* **2022**, *12*, 2103571. [CrossRef]
28. Bhatia, D.; Lee, K.-S.; Niazi, M.U.K.; Park, H.-S. Triboelectric nanogenerator integrated origami gravity support device for shoulder rehabilitation using exercise gaming. *Nano Energy* **2022**, *97*, 107179. [CrossRef]
29. Hwang, H.J.; Kim, J.S.; Kim, W.; Park, H.; Bhatia, D.; Jee, E.; Chung, Y.S.; Kim, D.H.; Choi, D. An ultra-mechanosensitive visco-poroelastic polymer ion pump for continuous self-powering kinematic triboelectric nanogenerators. *Adv. Energy Mater.* **2019**, *9*, 1803786. [CrossRef]
30. Cha, K.; Chung, J.; Heo, D.; Song, M.; Chung, S.-H.; Hwang, P.T.; Kim, D.; Koo, B.; Hong, J.; Lee, S. Lightweight mobile stick-type water-based triboelectric nanogenerator with amplified current for portable safety devices. *Sci. Technol. Adv. Mater.* **2022**, *23*, 161–168. [CrossRef]
31. Son, J.-H.; Heo, D.; Song, Y.; Chung, J.; Kim, B.; Nam, W.; Hwang, P.T.; Kim, D.; Koo, B.; Hong, J.; et al. Highly reliable triboelectric bicycle tire as self-powered bicycle safety light and pressure sensor. *Nano Energy* **2021**, *93*, 106797. [CrossRef]
32. Chung, J.; Heo, D.; Cha, K.; Lin, Z.-H.; Hong, J.; Lee, S. A portable device for water-sloshing-based electricity generation based on charge separation and accumulation. *Iscience* **2021**, *24*, 102442. [CrossRef]
33. Chung, J.; Song, M.; Chung, S.-H.; Choi, W.; Lee, S.; Lin, Z.-H.; Hong, J.; Lee, S. Triangulated Cylinder Origami-Based Piezoelectric/Triboelectric Hybrid Generator to Harvest Coupled Axial and Rotational Motion. *Research* **2021**, *2021*, 1–9. [CrossRef]
34. Chung, S.-H.; Chung, J.; Kim, B.; Kim, S.; Lee, S. Screw Pump-Type Water Triboelectric Nanogenerator for Active Water Flow Control. *Adv. Eng. Mater.* **2020**, *23*, 2000758. [CrossRef]
35. Dharmasena, R.D.I.G.; Silva, S. Towards optimized triboelectric nanogenerators. *Nano Energy* **2019**, *62*, 530–549. [CrossRef]
36. Hwang, H.J.; Hong, H.; Cho, B.G.; Lee, H.K.; Kim, J.S.; Lee, U.J.; Kim, W.; Kim, H.; Chung, K.-B.; Choi, D. Band well structure with localized states for enhanced charge accumulation on Triboelectrification. *Nano Energy* **2021**, *90*, 106647. [CrossRef]
37. Choi, J.H.; Ra, Y.; Cho, S.; La, M.; Park, S.J.; Choi, D. Electrical charge storage effect in carbon based polymer composite for long-term performance enhancement of the triboelectric nanogenerator. *Compos. Sci. Technol.* **2021**, *207*, 108680. [CrossRef]

38. Heo, D.; Chung, J.; Shin, G.; Seok, M.; Lee, C.; Lee, S. Yo-Yo Inspired Triboelectric Nanogenerator. *Energies* **2021**, *14*, 1798. [CrossRef]
39. Pan, M.; Yuan, C.; Liang, X.; Zou, J.; Zhang, Y.; Bowen, C. Triboelectric and Piezoelectric Nanogenerators for Future Soft Robots and Machines. *Iscience* **2020**, *23*, 101682. [CrossRef]
40. Lin, L.; Wang, S.; Xie, Y.; Jing, Q.; Niu, S.; Hu, Y.; Wang, Z.L. Segmentally Structured Disk Triboelectric Nanogenerator for Harvesting Rotational Mechanical Energy. *Nano Lett.* **2013**, *13*, 2916–2923. [CrossRef]
41. Zhao, L.; Zheng, Q.; Ouyang, H.; Li, H.; Yan, L.; Shi, B.; Li, Z. A size-unlimited surface microstructure modification method for achieving high performance triboelectric nanogenerator. *Nano Energy* **2016**, *28*, 172–178. [CrossRef]
42. Xu, W.; Wong, M.C.; Hao, J. Strategies and progress on improving robustness and reliability of triboelectric nanogenerators. *Nano Energy* **2018**, *55*, 203–215. [CrossRef]
43. Yang, B.; Tao, X.-M.; Peng, Z. Upper limits for output performance of contact-mode triboelectric nanogenerator systems. *Nano Energy* **2018**, *57*, 66–73. [CrossRef]
44. Zi, Y.; Wu, C.; Ding, W.; Wang, Z.L. Maximized Effective Energy Output of Contact-Separation-Triggered Triboelectric Nanogenerators as Limited by Air Breakdown. *Adv. Funct. Mater.* **2017**, *27*, 1700049. [CrossRef]
45. Jiang, C.; Dai, K.; Yi, F.; Han, Y.; Wang, X.; You, Z. Optimization of triboelectric nanogenerator load characteristics considering the air breakdown effect. *Nano Energy* **2018**, *53*, 706–715. [CrossRef]
46. Huang, J.; Fu, X.; Liu, G.; Xu, S.; Li, X.; Zhang, C.; Jiang, L. Micro/nano-structures-enhanced triboelectric nanogenerators by femtosecond laser direct writing. *Nano Energy* **2019**, *62*, 638–644. [CrossRef]
47. Xi, Y.; Zhang, F.; Shi, Y. Effects of surface micro-structures on capacitances of the dielectric layer in triboelectric nanogenerator: A numerical simulation study. *Nano Energy* **2020**, *79*, 105432. [CrossRef]
48. Yi, Z.; Liu, D.; Zhou, L.; Li, S.; Zhao, Z.; Li, X.; Wang, Z.L.; Wang, J. Enhancing output performance of direct-current triboelectric nanogenerator under controlled atmosphere. *Nano Energy* **2021**, *84*, 105864. [CrossRef]
49. Wang, J.; Wu, C.; Dai, Y.; Zhao, Z.; Wang, A.; Zhang, T.; Wang, Z.L. Achieving ultrahigh triboelectric charge density for efficient energy harvesting. *Nat. Commun.* **2017**, *8*, 88. [CrossRef]
50. Seol, M.-L.; Han, J.-W.; Moon, D.-I.; Meyyappan, M. Triboelectric nanogenerator for Mars environment. *Nano Energy* **2017**, *39*, 238–244. [CrossRef]
51. Wang, S.; Niu, S.; Yang, J.; Lin, L.; Wang, Z.L. Quantitative Measurements of Vibration Amplitude Using a Contact-Mode Freestanding Triboelectric Nanogenerator. *ACS Nano* **2014**, *8*, 12004–12013. [CrossRef]
52. Wang, Z.L. From contact-electrification to triboelectric nanogenerators. *Rep. Prog. Phys.* **2021**, *84*, 096502. [CrossRef]
53. Niu, S.; Wang, S.; Lin, L.; Liu, Y.; Zhou, Y.S.; Hu, Y.; Wang, Z.L. Theoretical study of contact-mode triboelectric nanogenerators as an effective power source. *Energy Environ. Sci.* **2013**, *6*, 3576–3583. [CrossRef]
54. Cho, H.; Chung, J.; Shin, G.; Sim, J.-Y.; Kim, D.S.; Lee, S.; Hwang, W. Toward sustainable output generation of liquid–solid contact triboelectric nanogenerators: The role of hierarchical structures. *Nano Energy* **2018**, *56*, 56–64. [CrossRef]
55. Chung, J.; Heo, D.; Kim, B.; Lee, S. Superhydrophobic Water-Solid Contact Triboelectric Generator by Simple Spray-On Fabrication Method. *Micromachines* **2018**, *9*, 593. [CrossRef] [PubMed]
56. Kim, B.; Chung, J.; Moon, H.; Kim, D.; Lee, S. Elastic spiral triboelectric nanogenerator as a self-charging case for portable electronics. *Nano Energy* **2018**, *50*, 133–139. [CrossRef]
57. Heo, D.; Kim, T.; Yong, H.; Yoo, K.T.; Lee, S. Sustainable oscillating triboelectric nanogenerator as omnidirectional self-powered impact sensor. *Nano Energy* **2018**, *50*, 1–8. [CrossRef]
58. Niu, S.; Liu, Y.; Wang, S.; Lin, L.; Zhou, Y.S.; Hu, Y.; Wang, Z.L. Theory of Sliding-Mode Triboelectric Nanogenerators. *Adv. Mater.* **2013**, *25*, 6184–6193. [CrossRef]
59. Niu, S.; Liu, Y.; Wang, S.; Lin, L.; Zhou, Y.S.; Hu, Y.; Wang, Z.L. Theoretical Investigation and Structural Optimization of Single-Electrode Triboelectric Nanogenerators. *Adv. Funct. Mater.* **2014**, *24*, 3332–3340. [CrossRef]
60. Shao, J.; Willatzen, M.; Wang, Z.L. Theoretical modeling of triboelectric nanogenerators (TENGs). *J. Appl. Phys.* **2020**, *128*, 111101. [CrossRef]
61. Chung, J.; Yong, H.; Moon, H.; Van Duong, Q.; Choi, S.T.; Kim, D.; Lee, S. Hand-Driven Gyroscopic Hybrid Nanogenerator for Recharging Portable Devices. *Adv. Sci.* **2018**, *5*. [CrossRef]
62. Kim, T.; Kim, D.Y.; Yun, J.; Kim, B.; Lee, S.H.; Kim, D.; Lee, S.J.N.E. Direct-current triboelectric nanogenerator via water electrification and phase control. *Nano Energy* **2018**, *52*, 95–104. [CrossRef]
63. Chung, J.; Yong, H.; Moon, H.; Choi, S.T.; Bhatia, D.; Choi, D.; Kim, D.; Lee, S. Capacitor-Integrated Triboelectric Nanogenerator Based on Metal-Metal Contact for Current Amplification. *Adv. Energy Mater.* **2018**, *8*, 1703024. [CrossRef]
64. Fontes, D.H.; Ribatski, G.; Filho, E.P.B. Experimental evaluation of thermal conductivity, viscosity and breakdown voltage AC of nanofluids of carbon nanotubes and diamond in transformer oil. *Diam. Relat. Mater.* **2015**, *58*, 115–121. [CrossRef]
65. Chung, J.; Chung, S.-H.; Lin, Z.-H.; Jin, Y.; Hong, J.; Lee, S. Dielectric liquid-based self-operating switch triboelectric nanogenerator for current amplification via regulating air breakdown. *Nano Energy* **2021**, *88*, 106292. [CrossRef]
66. Zhang, J.; Zheng, Y.; Xu, L.; Wang, D. Oleic-acid enhanced triboelectric nanogenerator with high output performance and wear resistance. *Nano Energy* **2019**, *69*, 104435. [CrossRef]
67. Zhou, L.; Liu, D.; Zhao, Z.; Li, S.; Liu, Y.; Liu, L.; Gao, Y.; Wang, Z.L.; Wang, J. Simultaneously Enhancing Power Density and Durability of Sliding-Mode Triboelectric Nanogenerator via Interface Liquid Lubrication. *Adv. Energy Mater.* **2020**, *10*. [CrossRef]

68. Wang, K.; Li, J.; Li, J.; Wu, C.; Yi, S.; Liu, Y.; Luo, J. Hexadecane-containing sandwich structure based triboelectric nanogenerator with remarkable performance enhancement. *Nano Energy* **2021**, *87*, 106198. [CrossRef]
69. Chung, S.H.; Chung, J.; Song, M.; Kim, S.; Shin, D.; Lin, Z.H.; Koo, B.; Kim, D.; Hong, J.; Lee, S. Nonpolar Liquid Lubricant Submerged Triboelectric Nanogenerator for Current Amplification via Direct Electron Flow. *Adv. Energy Mater.* **2021**, *11*, 2100936. [CrossRef]
70. Song, M.; Chung, J.; Chung, S.-H.; Cha, K.; Heo, D.; Kim, S.; Hwang, P.T.; Kim, D.; Koo, B.; Hong, J.; et al. Semisolid-lubricant-based ball-bearing triboelectric nanogenerator for current amplification, enhanced mechanical lifespan, and thermal stabilization. *Nano Energy* **2021**, *93*, 106816. [CrossRef]
71. Zhu, D.; Hu, Y.-Z. The study of transition from elastohydrodynamic to mixed and boundary lubrication. The advancing frontier of engineering tribology. In Proceedings of the 1999 STLE/ASME HS Cheng Tribology Surveillance, New York, NY, USA; 1999; pp. 150–156.
72. Jin, Z.; Fisher, J. Tribology in Joint Replacement. In *Joint Replacement Technology*; Elsevier: Amsterdam, The Netherlands, 2014; pp. 31–61.
73. Höglund, E. Influence of lubricant properties on elastohydrodynamic lubrication. *Wear* **1999**, *232*, 176–184. [CrossRef]
74. Prata, A.T.; Barbosa, J.R., Jr. Role of the thermodynamics, heat transfer, and fluid mechanics of lubricant oil in hermetic reciprocating compressors. *Heat Transf. Eng.* **2009**, *30*, 533–548. [CrossRef]
75. Kitamura, T.; Kojima, H.; Hayakawa, N.; Kobayashi, K.; Kato, T.; Rokunohe, T. Influence of space charge by primary and secondary streamers on breakdown mechanism under non-uniform electric field in air. In Proceedings of the 2014 IEEE Conference on Electrical Insulation and Dielectric Phenomena (CEIDP), Des Moines, IA, USA, 19–22 October 2014; pp. 122–125. [CrossRef]
76. Li, Y.; Zhao, Z.; Liu, L.; Zhou, L.; Liu, D.; Li, S.; Chen, S.; Dai, Y.; Wang, J.; Wang, Z.L. Improved Output Performance of Triboelectric Nanogenerator by Fast Accumulation Process of Surface Charges. *Adv. Energy Mater.* **2021**, *11*, 2100050. [CrossRef]
77. Zhang, C.; Zhou, L.; Cheng, P.; Yin, X.; Liu, D.; Li, X.; Guo, H.; Wang, Z.L.; Wang, J. Surface charge density of triboelectric nanogenerators: Theoretical boundary and optimization methodology. *Appl. Mater. Today* **2019**, *18*, 100496. [CrossRef]
78. Wang, S.; Xie, Y.; Niu, S.; Lin, L.; Liu, C.; Zhou, Y.S.; Wang, Z.L. Maximum Surface Charge Density for Triboelectric Nanogenerators Achieved by Ionized-Air Injection: Methodology and Theoretical Understanding. *Adv. Mater.* **2014**, *26*, 6720–6728. [CrossRef] [PubMed]
79. Gonda, A.; Capan, R.; Bechev, D.; Sauer, B. The Influence of Lubricant Conductivity on Bearing Currents in the Case of Rolling Bearing Greases. *Lubricants* **2019**, *7*, 108. [CrossRef]
80. Liu, X.; Zhang, J.; Zhang, L.; Feng, Y.; Feng, M.; Luo, N.; Wang, D. Influence of interface liquid lubrication on triboelectrification of point contact friction pair. *Tribol. Int.* **2021**, *165*, 107323. [CrossRef]
81. Wang, Y.; Wang, T.; Da, P.; Xu, M.; Wu, H.; Zheng, G. Silicon Nanowires for Biosensing, Energy Storage, and Conversion. *Adv. Mater.* **2013**, *25*, 5177–5195. [CrossRef]
82. Wang, Y.; Narayanan, S.R.; Wu, W. Field-Assisted Splitting of Pure Water Based on Deep-Sub-Debye-Length Nanogap Electrochemical Cells. *ACS Nano* **2017**, *11*, 8421–8428. [CrossRef]
83. Wu, J.; Xi, Y.; Shi, Y. Toward wear-resistive, highly durable and high performance triboelectric nanogenerator through interface liquid lubrication. *Nano Energy* **2020**, *72*, 104659. [CrossRef]